Available online at www.sciencedirect.com
SCIENCE DIRECT®
Computational Materials Science 33 (2005) 276–281
COMPUTATIONAL MATERIALS SCIENCE
www.elsevier.com/locate/commatsci

Ab initio simulations on AgCl(1 1 1) surface and AgCl(1 1 1)/α-Al_2O_3(0 0 0 1) interface

Yu.F. Zhukovskii [a,*], E.A. Kotomin [a,b], Yu. Mastrikov [b], J. Maier [b]

[a] *Institute for Solid State Physics, University of Latvia, Kengaraga str. 8, Riga LV-1063, Latvia*
[b] *Max Planck Institut für Festkörperforschung, Heisenbergstr. 1, Stuttgart D-70569, Germany*

Abstract

The defect chemistry and ionic transport properties of the AgCl(1 1 1)/α-Al_2O_3(0 0 0 1) interface were considered by using ab initio slab calculations. These calculations were performed in the framework of plane-wave basis set combined with the density functional theory (DFT), as implemented into the VASP computer code, and Gaussian basis set combined with the Hartree–Fock method (CRYSTAL-98 code). We analyze the electron density distribution on the interface and the electrostatic potential distribution near the AgCl surface. The size of the silver ion is too great to enter the corundum surface layer and to create excess silver ions in this way. This is in agreement with the experiments on heterogeneous doping of AgCl revealing α-alumina to be inactive compared with γ-alumina. The energy to thermally create a vacancy in the first layer at the expense of an interstitial ion is large compared with the bulk Frenkel energy. Despite the calculated low activation energy for vacancy transport in the first layer ($\Delta H_s^{\#} = 0.23$ eV), the vacancy concentration will be too small to generate perceptible surface conductivity. The striking similarity of $\Delta H_s^{\#}$ with the bulk value is due to the quite symmetrical arrangement of the considered interface.

1. Introduction

Striking ionic conductivity enhancements were experimentally observed at the interfaces between ion conducting solids, such as LiCl, AgCl, AgBr, TlCl, CaF_2, etc., and insulating oxides such as alumina or silica substrates [1–3]. This topic remains of great relevance for catalysis, electrode kinetics, photography, and sensor technology. As far as cation conductors are concerned, alumina is more active than silica owing to its higher surface basicity. Regarding alumina modifications, γ-alumina is very active, while α-alumina seems to be only active if contaminated with water. Recently, similar enhancement effects were found for oxide/polymer

* Corresponding author.
E-mail address: j.zhukovskij@fkf.mpg.de (Yu.F. Zhukovskii).

0927-0256/$ - see front matter © 2005 Elsevier B.V. All rights reserved.
doi:10.1016/j.commatsci.2004.12.046

electrolyte or even oxide/liquid electrolyte system [4,5].

Most of studies on the enhanced ionic conductivity performed so far considered two-phase conducting system at the phenomenological level [6]. In a line with the model of 'heterogeneous doping' [1] developed as a quantitative basis to explain conductivity effects, the reason for the conductivity enhancement in the interfacial region turned out to be the increase in the mobile silver vacancy concentration in the interfacial layer [2]. Atomistic, molecular dynamic (MD) simulations have been performed on the LiI(001) & (002)/α-Al_2O_3(0001) and LiI(001) & (002)/γ-Al_2O_3(001) interfaces [7]. (This method was used for the simulation of Na^+ conductivity in β-alumina [8]). The activation energy of Li^+ ion migration on both interfaces was found to be the same, 0.38 eV. The main reason for the enhanced conductivity was indeed shown to be the migration of metal (Li) vacancies formed as a consequence of Li^+ penetration into the alumina surface plane, with γ-alumina to be more active then α-alumina.

In this study, we perform first comparative ab initio slab simulations on both AgCl(111) substrate and AgCl/α-Al_2O_3(0001) interface. Initially, the optimal interfacial configurations as well as basic properties of both corundum substrate and silver chloride adsorbate were estimated by us using ab initio Hartree–Fock (HF) and density functional theory (DFT) formalisms applied for the localized atomic orbitals, as implemented into the CRYSTAL-98 computer code [9]. In order to improve the quality of geometry optimization, we have employed also the Vienna ab initio simulation package (VASP) [10] performing plane-wave DFT calculations using ultra-soft Vanderbilt pseudopotentials (US-PP).

2. Theoretical

When performing CRYSTAL calculations [9] (see details for the Ag/α-Al_2O_3(0001) interface in Ref. [11]), one should correctly choose Gaussian-type basis sets (BSs) for the localized, atomic wave functions. The BSs for Ag and Cl [12] were optimized using small and large core Hay–Wadt pseudopotentials [13], i.e. HWSC-311(sp)-31(d) and HWLC-31(sp), respectively. For corundum, we have used the all-valence Al and O basis sets 8(s)-511(sp)-1(d) and 8(s)-411(sp)-1(d), respectively [14]. We have performed partial re-optimization of the outermost shells of all BSs mentioned above, using the ParOptimize code [15] interfaced with CRYSTAL-98. It implements conjugated gradients optimization technique [16] with a numerical computation of derivatives. ParOptimize code has been also used by us for the geometry optimization of two-dimensional (2D) slab models of both AgCl(111) surface and AgCl/α-Al_2O_3-(0001) interface.

When using the VASP package [10,17], one performs an iterative solution of the Kohn–Sham equations based on residuum-minimization and optimized charge-density mixing routines [18]. In the present calculations, we use the LDA (local density approximation) exchange–correlation functional based on the quantum Monte Carlo calculations of Ceperley and Alder, as parameterized by Perdew and Zunger [19]. The electronic states are expanded into plane waves; the electron–ion interaction is described in terms of ultrasoft pseudopotentials [20,21]. The VASP computational procedure includes the calculations of the Hellmann–Feynman forces acting on the atoms and of the stresses on the unit cell (UC). The total energy is optimized with respect to the positions of the atoms within UC. The kinetic energy cutoff, which determines the whole set of plane waves with smaller energy included in the basis set, has been chosen to be $E_{cut} = 395.7$ eV. The Brillouin zone integrations have been performed in the grid of $4 \times 4 \times 2$ k-point set.

The AgCl(111) substrate has been modeled using slabs of different thickness, with even (both Ag- and Cl-terminated) and odd (Ag-terminated) number of layers varied from 2 to 19. The perfect AgCl(111) surface belongs to the symmetry group C_{3v} which is spatially compatible with the hexagonal plane group D_3^2 of α-Al_2O_3(0001) surface (its optimized structure was described by us in Ref. [11]): the C_{3v} rotation axes normal to the (0001) surface contain Al^{3+} ions and form a regular (111) network. In VASP calculations, we have mainly considered 6 layers separated by the

optimized vacuum gaps along the vertical, z-axis of similar thickness. In order to simulate the AgCl/α-Al_2O_3(0 0 0 1) interface, we have used nine-layer slab for corundum substrate consisting of three oxygen and six aluminum layers (Fig. 1) as well as four-layer slab for the one-side AgCl(1 1 1) adsorbate atop α-Al_2O_3 (0 0 0 1). Thickness of the vacuum gap has been chosen also compatible with thickness of the interface slab.

Surface lattice parameter mismatch between the AgCl(1 1 1) adsorbate ($r^{(min)}_{Ag-Ag} = 3.908$ Å [12]) and Al-terminated α-Al_2O_3(0 0 0 1) substrate (minimal distance between adjacent Al^{3+}-axes $a_{corundum}/\sqrt{3} = 2.751$ Å [14]) forces adsorbate layer, as a more soft interface component, to modify its structure to the suitable stable configuration. The structure of corundum substrate has been considered as rigid, except for the position of the outer Al^{3+} ions. To allow the outward migration of silver ions, we have simulated a partial occupation of outermost AgCl planes, using 1/3 monolayer (ML) as shown in Fig. 1. Such 'loose' adsorbate morphology makes easier its structural relaxation, to overcome interfacial lattice parameter mismatch. Ionic positions have been determined during the VASP procedure of geometry optimization.

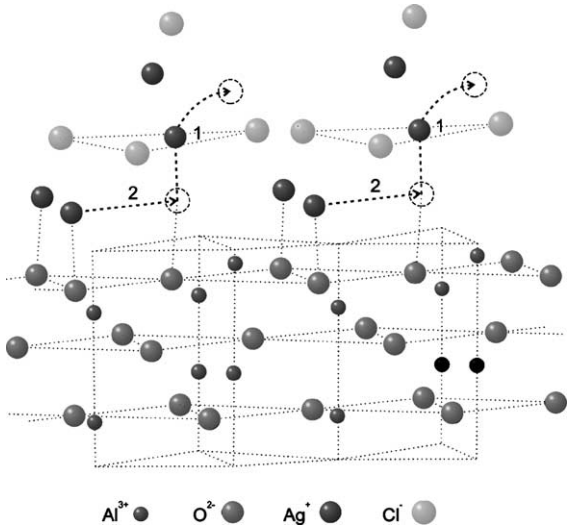

Fig. 1. Side view of one-sided slab model of the AgCl/α-Al_2O_3(0 0 0 1) interface, where optimized configuration of the silver chloride substrate (4/3 ML for both Ag^+ and Cl^- ions) is positioned by the lower Ag^+ ions towards the outermost O^{2-} ions of the corundum substrate as shown by dot lines. When modeling diffusion, we first move one of the interfacial Ag^+ ions outwards (trajectory 1) and then an internal migration of the Ag^+ ions is simulated (trajectory 2). Images of adjacent oxygen ions positioned on the same substrate layers are joined by dotted lines. This is also true for Al^{3+} ions.

3. Modeling of AgCl(1 1 1) surface and AgCl/α-Al_2O_3(0 0 0 1) interface

When optimizing geometry of thin AgCl(1 1 1) slabs, we observe the growth of its lattice constant synchronously with the inward relaxation of the outer layers. The thicker the slab of silver chloride, the smaller these changes, thus approaching to the bulk-like (1 1 1)-terminated AgCl. We calculated also the electrostatic potential distributions across the slabs, $\overline{U}(z)$, averaged over given crystalline plane. Calculations show that for the Ag-terminated surface of 18-layer slab $\overline{U}(z)$ exceeds that in the bulk by 0.22 V. On the other hand, the potential on the Cl-terminated surface is smaller than in the bulk by 0.88 V. The latter results qualitatively agree with the experimental data [22] indicating the potential varies with the temperature from −0.1 V down to −0.3 V. The difference with calculated potential could be attributed partly to the divalent impurity segregation observed in these experiments. The calculated value of $\overline{U}(z)$ rapidly decays to the vacuum, typically within one-two interplane distances.

There are 12 possible positions how Ag^+ ions could sit atop the ions of substrate (Fig. 2). Total energy minimum has been found for the Ag^+ ions

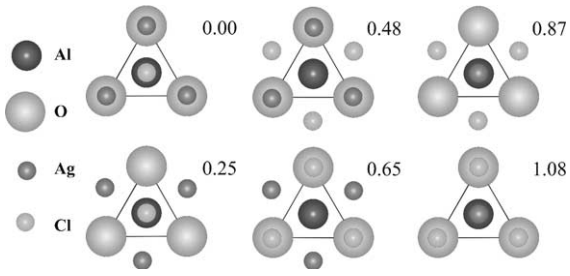

Fig. 2. Six possible arrangements of Ag^+ and Cl^- ions over the corundum substrate. The corresponding numbers give relative energies of the position stability.

atop the outermost O^{2-} ions of corundum, whereas Cl^- ions are lying upon Al^{3+}-axes over interfacial Ag^+-sublayer (Fig. 1). This result qualitatively confirms the conclusion recently made in experimental study of the $CuCl_2(1\,1\,1)/\gamma$-Al_2O_3-$(1\,1\,0)$ interface [23] that metal ions are positioned closer to the alumina substrate than Cl^- ions, which are localized atop the Al^{3+} axis. To arrange Ag^+ and Cl^- ions analogously to that as shown in Fig. 1, the adsorbate geometry should be particularly 'stepped', taking into account lattice parameter mismatch mentioned above.

Let us consider now results of the VASP calculations on the Ag^+ ion migration on both AgCl(1 1 1) substrate and on the AgCl/α-Al_2O_3(0 0 0 1) interface, which is the most important stage to clarify the reason of enhanced Ag^+ ion conductivity in the interface. As a first step of both simulations, we simulated silver ion motion through the nearest chlorine triangle outside the interfacial AgCl bilayer (trajectory 1 in Fig. 1). For this purpose, we consider six-layer AgCl(1 1 1) slab where outermost silver chloride bilayer possess 'loose' structure as shown in Fig. 1. As a result, we find the energy barriers per ion for outwards Ag^+ diffusion to be very low for 'the pure loose' AgCl slab and quite large (>4 eV) for the AgCl/α-Al_2O_3(0 0 0 1) interface, respectively. Obviously, the former structure is unstable with respect to the expansion. On the contrary, for the AgCl/corundum interface, the optimized 'loose' structure of the outermost adsorbate bilayer more correctly describes silver chloride overlayer than the flat surface, due to interfacial lattice parameter mismatch.

One of key results of this study is the activation barriers of Ag^+ vacancy migration parallel to the AgCl/corundum interface (trajectory 2 in Fig. 1) which is 0.23 eV. Surprisingly, the latter interfacial activation energy coincides with the experimental value for AgCl bulk. It may, however, find its explanation in the rather symmetrical 'bicrystal' arrangement. It is obvious from Fig. 1, that both the Ag^+ ion as well as the vacancy see similar surroundings in both crystal halves as far as Coulomb effect is concerned, which follows from Fig. 3. Polarizability of Ag^+ ions thus should result in a roughly constant variation of the energy profile

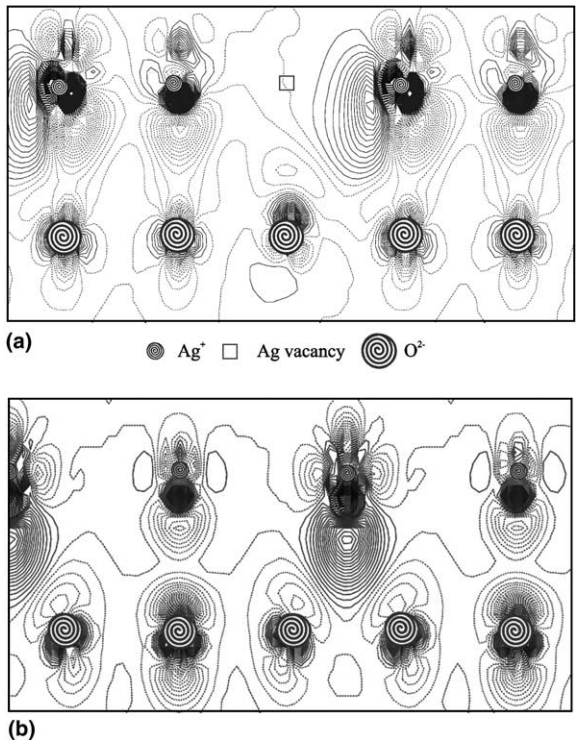

Fig. 3. 2D Difference electron charge density distributions (the total electron density minus the sum of electron densities of isolated silver chloride and corundum slabs) along the $(10\bar{1}0)$ section plane of the AgCl/α-Al_2O_3(0 0 0 1) interface: (a) equilibrium vacancy position, and (b) saddle point of the Ag^+ ion diffusion. Dash-dot isolines correspond to zero level. Solid and dash isolines describe positive and negative values of electron density, respectively. Isodensity increment is 0.002 e Å^{-3}.

along the reaction coordinate. Note also that migration energy of 0.23 eV is also quite compatible with molecular dynamic simulations for Li^+ ion migration on the LiI/Al_2O_3 interface (0.38 eV [7]). To clarify the value of energy barrier for Ag^+ ion diffusion we have also studied the analogous migration along a (1 1 1) plane in the AgCl bulk, with a lower silver vacancies concentration, using the $3 \times 3 \times 3$ extended UC for this purpose. The corresponding migration barrier was found to be 0.49 eV. This exceeds the experimental value (0.3 eV [1]) due to artificial localization of extra electron, released after creation of neutral silver vacancy at adjacent chlorine ion. The additional repulsion energy induced by the newly-formed dipole is estimated to be ~0.2 eV. Subtracting this

value from 0.49 eV, we achieve good quantitative agreement with experimental data for the barrier of Ag^+ ion migration in the bulk AgCl. In general, qualitative comparison of the migration barriers clearly shows strong influence of the corundum substrate on the Ag^+ vacancy mobility.

We can also illustrate our calculations for silver ion diffusion on the AgCl/corundum interface by the plots of the difference charge density distributions. Fig. 3a shows that both interfacial Ag^+ and O^{2-} ions are considerably polarized. Moreover, the polarization of area around the silver vacancy is strongly asymmetric, i.e., the induced electronic density localized on vacancy is shared with only one of three neighboring Ag^+ ions. Just this 'shared' Ag^+ ion can migrate towards the vacancy with a low activation barrier mentioned above, 0.23 eV. In the saddle-point position of jumping Ag^+ ion (Fig. 3b), it interacts considerably with both nearest O^{2-} ions across the interface. In this case, the induced electron density distribution in the interfacial area is much more uniform as compared to Fig. 3a. However, no significant charge transfer is observed. Both excess of the electronic density on the regular vacancy (0.23 e) and its deficiency on both neighboring vacancies around Ag^+ ion (−0.24 e) are caused by the charge re-distribution inside the AgCl adsorbate.

Unlike the smaller Li^+ ion, Ag^+ is not able to penetrate into the dense (0 0 0 1) surface of corundum and thus increase, in this way, the vacancy concentration in the interfacial AgCl sublayers. This is in agreement with the inactivity of dry α-Al_2O_3 in heterogeneously doping of AgCl. (It is however worth to mention that we did not check the injection of Ag^+ into interstitial site of the AgCl contact layer as a vacancy generation mechanism). Next studies have to show, how far the more open and active γ-Al_2O_3 or the contamination of H_2O on alumina to form hydroxyl groups changes the obtained results.

4. Summary

First principles calculations on slab models of both AgCl(1 1 1) substrate and AgCl/α-Al_2O_3-(0 0 0 1) interface, performed using ab initio CRYSTAL-98 and VASP packages, show that the most probable configuration of the interface between the silver chloride and α-corundum is a down-directed adsorbate Ag^+ sublayer sitting atop the outermost substrate O^{2-} ions, whereas the adsorbate Cl^- ions are initially placed atop the Al^{3+}-axes of the corundum substrate above the interfacial Ag^+ ions. The silver vacancy considerably polarizes both nearest in-plane Ag^+ ions and outermost O^{2-} ions across the interface. Migrating silver ion is strongly polarized towards the two nearest oxygen ions. The calculated energy barrier (0.23 eV) of the Ag^+ vacancy migration parallel to the AgCl/corundum interface practically coincides with the experimental value for bulk transport, which may be due to the symmetrical bicrystal arrangement in both cases. In a line with the experiments [1], the interface should not show perceptible excess conductivity for the two following reasons: (i) Ag^+ ions are not strongly adsorbed on the interface to α-Al_2O_3. Hence, an appreciable space charge conductivity is not expected; (ii) owing to the calculated high formation energy of Ag^+ vacancies on the surface layer, the proper surface conductivity should be small in spite of a small migration barrier.

Acknowledgements

This study was partly supported by the German–Israeli (GIF) grant Nr G-703.41.10 (YM). YZ thanks the Department of Physical Chemistry of the Max-Planck-Institute for Solid State Researches, Stuttgart, for warm hospitality during his visit there. The authors kindly thank J. Fleig for fruitful discussions, as well as D. Gryaznov for technical assistance.

References

[1] J. Maier, Prog. Solid State Chem. 23 (1995) 171.
[2] U. Riedel, J. Maier, R.J. Brook, J. Eur. Ceram. Soc. 9 (1992) 205.
[3] C.C. Liang, J. Electrochem. Soc. 120 (1973) 1289.
[4] A.J. Bhattacharyya, J. Maier, Adv. Mater. 16 (2004) 811.
[5] B. Scrosati, Applications of Electroactive Polymers, Chapman and Hall, London, 1993.

[6] J. Maier, J. Phys. Chem. Solids 46 (1985) 309.
[7] R.W.J.M. Huang Foen Chung, S.W. de Leeuw, J. Electroanal. Chem., in press.
[8] J.V.L. Beckers, K.J. van der Bent, S.W. de Leeuw, Solid State Ionics 133 (2000) 217.
[9] V.R. Saunders, R. Dovesi, C. Roetti, M. Causá, N.M. Harrison, R. Orlando, C.M. Zicovich-Wilson, CRYSTAL-98 User Manual, University of Turin, 1999.
[10] G. Kresse, J. Furthmüller, VASP Guide, University of Vienna, Austria, 2003.
[11] Yu.F. Zhukovskii, E.A. Kotomin, B. Herschend, K. Hermansson, P.W.M. Jacobs, Surf. Sci. 513 (2002) 343.
[12] E. Aprá, E.V. Stefanovich, R. Dovesi, C. Roetti, Chem. Phys. Lett. 186 (1991) 329.
[13] P.J. Hay, W.R. Wadt, J. Chem. Phys. 82 (1985) 284.
[14] M. Catti, G. Valerio, R. Dovesi, M. Causá, Phys. Rev. B 49 (1994) 14179.
[15] E. Heifets, R.I. Eglitis, E.A. Kotomin, J. Maier, G. Borstel, Phys. Rev. B 64 (2001) 235417.
[16] W.H. Press, S.A. Teukolsky, W.T. Vetterling, B.P. Flannery, Numerical Recipes in Fortran 77, Cambridge University Press, Cambridge, 1997.
[17] G. Kresse, J. Hafner, Phys. Rev. B 48 (1993) 13115; Phys. Rev. B 49 (1994) 14521.
[18] G. Kresse, J. Furthmueller, Comput. Math. Sci. 6 (1996) 15;
Phys. Rev. B 55 (1996) 11961.
[19] J.P. Perdew, A. Zunger, Phys. Rev. B 23 (1981) 5048.
[20] D. Vanderbilt, Phys. Rev. B 41 (1990) 7892.
[21] G. Kresse, J. Hafner, J. Phys.: Condens. Matter 6 (1994) 8245.
[22] S.K. Wonnell, L.M. Slifkin, Phys. Rev. B 48 (1993) 78.
[23] G. Leofanti, M. Padovan, M. Garilli, D. Carmello, A. Zecchina, G. Spoto, S. Bordiga, G. Turnes Palomino, C. Lamberti, J. Catal. 189 (2000) 91.